J Sol-Gel Sci Technol (2008) 47:290–299
DOI 10.1007/s10971-008-1786-0

ORIGINAL PAPER

Nonisocyanate based polyurethane/silica nanocomposites and their coating performance

Oğuz Türünç · Nilhan Kayaman-Apohan · M. Vezir Kahraman · Yusuf Menceloğlu · Atilla Güngör

Received: 12 February 2008 / Accepted: 2 June 2008 / Published online: 17 June 2008

Abstract A series of silica nano-particles with different size were prepared by sol–gel technique, then surface modification by using cyclic carbonate functional organoalkoxysilane (CPS) was performed. Various amounts of carbonated silica particles directly added into carbonated soybean oil (CSBO) and carbonated polypropylene glycol (CPPG) resin mixture to prepare polyurethane–silica nanocomposite coating compositions by nonisocyanate route using an aliphatic diamine as a curing agent. Cupping, gloss, impact, and taber abrasion tests were performed on aluminum panels coated with those nanocomposite formulations and tensile tests, thermogravimetric and SEM analyses were conducted on the free films prepared from the same coating formulations. An increase in abrasion resistance of CSBO-CPPG resin combination with the addition of silica was observed. In addition, the maximum weight loss of CSBO-CPPG resin combination was shifted to higher temperatures with incorporation of silica nano-particles The positive effect of modified silica particles on thermal stability of CSBO-CPPG system could be explained in such a way that PPG chains are able to disperse particles in the medium throughout the interactions between ether linkages and silanol groups.

Keywords Silica · Nonisocyanate polyurethane · Nanocomposite · Cyclic carbonate

O. Türünç · N. Kayaman-Apohan (✉) · M. V. Kahraman · A. Güngör
Department of Chemistry, Marmara University, 34722 Göztepe-Istanbul, Turkey
e-mail: napohan@marmara.edu.tr

Y. Menceloğlu
Faculty of Engineering and Natural Sciences, Sabancı University, 34956 Tuzla-Istanbul, Turkey

1 Introduction

In recent years, the development of polymer nanocomposites has offered promise for yielding materials with excellent performances compared to conventional composites [1]. They represent a new class of composite materials, where an inorganic phase is dispersed at a nanoscale level into a polymeric matrix; among them polymer–SiO_2, polymer–TiO_2 and polymer–clay nanocomposites are within the most searched [2–6]. The early works on nanocomposite materials demonstrated that the enhancement of mechanical and thermomechanical properties is definitely higher in the case of nanosized fillers with respect to micron-sized dispersed. [7, 8] In case the ultra-fine phase dimensions of the nanoparticles are maintained, such nanocomposites are much lighter in weight, transparent and easier to be processed than conventional inorganic particulate filled polymers since they possess a significant improvement in both rigidity and toughness. [9] In addition, they also acquire some special properties like barrier properties towards gases [10] and reduction of flammability. [11] As the nano-scale morphology plays an important role in achieving desired and tunable macroscopic properties, to obtain a better compatibility between the filler and the host polymeric materials is necessary [12]. The surface modification of the inorganic nanoparticles by using acrylic/vinylic or epoxy functional trialkoxysilanes is recommended [13]. The formation of chemical bonds between the inorganic and organic components is expected to be of great importance to guarantee a durable chemical junction between the two incompatible phases [14–17].

Polyurethanes (PU) produced with conventional methods are used world wide on a large scale for foam, fiber, adhesive and coating applications so forth. They are synthesized via the reaction between isocyanate oligomers and

polyol oligomers. During this process, inevitable use of isocyanates makes polyurethane production quite toxic and dangerous. Despite the extremely toxic nature of isocyanates, polyurethanes made enormous market penetration following the second world war. Especially, the extreme flexibility in the production of polyether polyols with different structures was the distinct reason behind this tremendous market gain of PU. Early days of the introduction of polyurethanes, available technology and attraction of production cost were the prime factors for a commercial success. However, in the last two decade; harmony between technology, economy and ecology became dictating factor introduction of new methods and materials. In this sense, cyclic carbonates are a class of materials drawing attention for their potential use in environmental-friendly PU technology [18]. Cyclic carbonates can be synthesized from epoxy compounds or oligomers [19–31]. Network or linear non-isocyanate polyurethanes are synthesized by the reaction of cyclic carbonates with aliphatic diamines [32–38]. This reaction produce neither volatile nor non-volatile by-product, but do produce intermolecular hydrogen bridges at which the susceptibility of the polymer back-bone to hydrolyze lowers. The lethal dose of meta-xylene diamine which is the most toxic diamine compound used in non-isocyanate polyurethane production is 20–40 times lower than that of the most used polyisocyanate, diphenylmethane diisocyanate [39].

The main objective of this work is to development of environmentally friendly polyurethane–silica nanocomposite coatings with good thermal and mechanical properties. To accomplish this aim, a novel cyclic carbonate functional organoalkoxysilane (CPS) coupling agent was synthesized and used for the modification of silica particle surface. The cyclic-carbonate functional resins and modified silica particles were used to prepare nanocomposite coating formulations with 0–4 wt% silica content. Finally the formulations were cured with a diamine to form nano-composite coatings by means of a non-isocyanate route. Cupping, gloss, impact, and Taber abrasion tests were performed on aluminum panels coated with those nano-composite formulations and tensile tests, DCS, TGA and SEM analyses were conducted on the free films prepared from the same coating formulations.

2 Experimental

2.1 Materials

Epoxidized soybean oil (ESBO) with 4.10 epoxy groups per triglyceride molecule was kindly supplied from Cognis Turkey. Polypropyleneglycol diglycidylether (PPG-DGE) with a molecular weight of 640 g/mol, 3-Glycidyloxypropyl trimethoxysilane (GPTMS) and Tetrabutylammonium bromide (TBAB) were purchased from Sigma-Aldrich. Tetraethylorthosilicate (TEOS), pyridine and butylenediamine (BDA) were purchased from Merck AG. BYK-331 was obtained from BYK Chemie. Carbondioxide was used after passage through a silica gel column. All other chemicals were of analytical grade and were purchased from Merck AG. Anode oxidized aluminum panels (75 mm × 150 mm × 0.82 mm) were used as substrates in all coating applications.

2.2 Synthesis

2.2.1 Preparation of silica particles

The silica sols were obtained from five different formulations given in the Table 1 according to Ströber method [40]. TEOS and half volume of ethanol were charged into a round-bottom flask and heated to 50 °C. Then ammonia, water and the remaining half of ethanol were added and stirred magnetically for 10 h at the same temperature. The TEOS was hydrolyzed to form $Si(OH)_4$ which then condensed to form silica particles. The silica particles were washed with dichloromethane and dried at 110 °C before being used in the polyurethane matrix.

2.2.2 Carbonate functionalization of silica particles

GPTMS with 5 wt% of TBAB catalyst was charged into a round-bottom reactor and heated to 110 °C in CO_2 stream and stirred for 24 h. The reactor was then cooled to room temperature, unreacted CO_2 was vented out, catalyst was separated by centrifugation. Then, carbonate functional silane coupling agent (4-((3-(trimethoxysilyl)propoxy) methyl)-1,3-dioxolan-2-one, CPS) and silica particles having M4 formulation were mixed and stirred for further 20 h at 65 °C. Then, the non-bonded CPS was removed by centrifuge and dichloromethane extraction. A representation of this reaction is shown in Scheme 1.

Table 1 Silica sol formulations

	M1	M2	M3	M4	M5
TEOS (mmol)	10.0	10.0	10.0	10.0	10.0
C_2H_5OH (mmol)	165.0	165.0	165.0	165.0	165.0
NH_3 (mmol)	6.0	6.0	4.0	10.0	5.0
H_2O (mmol)	40.0	80.0	80.0	20.0	80.0
Partical size (nm)	237 ± 86	321 ± 29	194 ± 55	165 ± 31	275 ± 45

Scheme 1 Synthesis of Carbonate Functional Silica Particles (M4CPS)

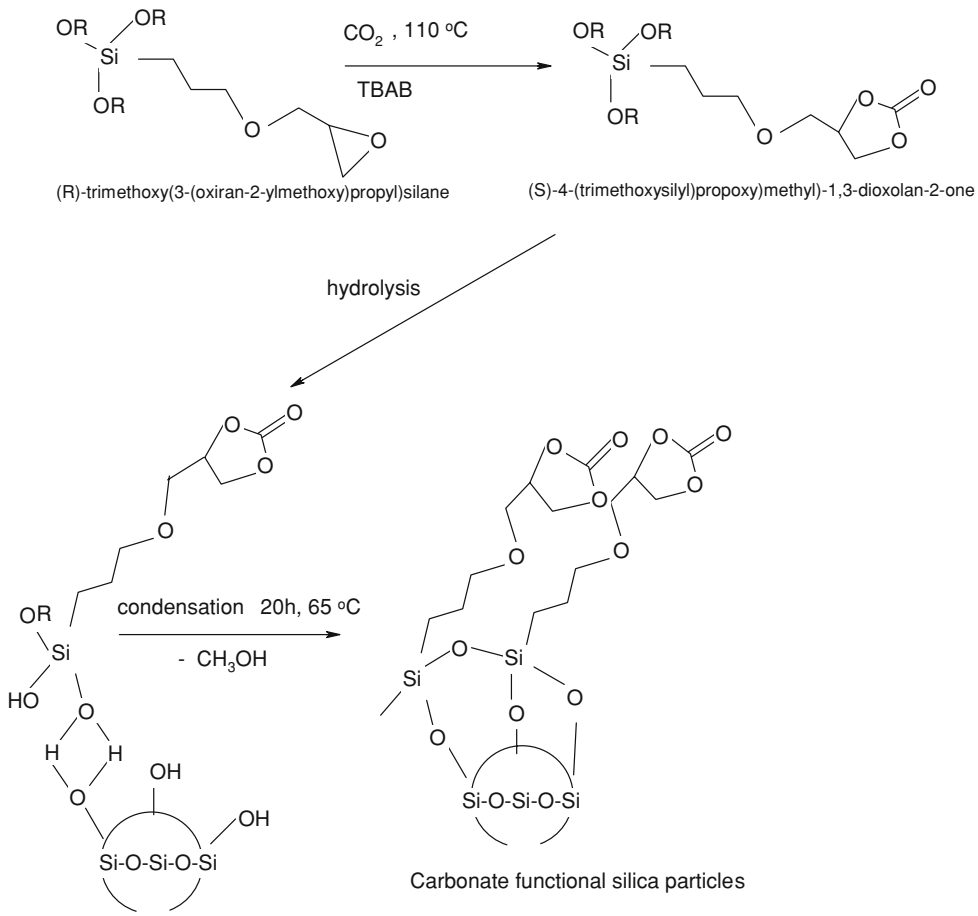

2.2.3 Carbonate modification of epoxy resins

In this stage, two different type of epoxy resins were used; ESBO and PPG-DGE. The modification of ESBO was performed in a closed vessel at 110 °C and 65 psi CO_2 by TBAB catalysis for 12 h, whereas the modification of PPG-DGE was performed in supercritical conditions (1,500 psi) at 80 °C in 48 h using the same catalyst. A representation of this reaction is shown in Scheme 2.

2.2.4 Preparation of polyurethane−silica nanocomposite coatings and free films by non-isocyanate route

The various amounts of silica particles were added into ethanol, pyridine (as catalyst) and BYK (as wetting agent) mixture and kept in a sonication bath for 30 min. Then a known amount of carbonate modified resins (CSBO and CPPG) were added into the formulation and mixed thoroughly at 150 rpm for 10 min until become clear and homogeneous . Finally BDA was added as a hardener and stirred 10 min additionally. The composition of all coating formulations is given in Table 2. In order to remove air bubbles formed during mixing; the beaker content heated to 35 °C then kept under gentle vacuum for 10 min without upsetting the composition. After removal of air bubbles, the prepared formulations were applied on to aluminum panels using a wire gauged bar applicator in order to obtain uniform thickness of 30 μm and left at 75 °C for 24 h to cure.

Moreover, hybrid free films were prepared by pouring the liquid formulations on to a Teflon™ mold (10 mm × 50 mm × 1 mm) and cured at 75 °C.

2.3 Characterization

FT-IR spectra were recorded on Shimadzu 8300 FT-IR spectrometer. The solid state cross-polarization (CP)/magic-anglespinning (MAS) NMR spectra were recorded using a Varian Unity Inova spectrometer operated at 500 MHz. SEM (Scanning Electron Microscope) imaging was performed on a JEOL-JSM-5919LV. SEM micrographs were taken by dropping sols on carbon platform and drying under vacuum before gold-sputtering. Thermogravimetric analyses (TGA) were conducted with Netzsch STA 409 CD while nitrogen purging using a heating rate of 10 °C/min over the temperature range of ca. ambient to 750 °C. Differential Scanning calorimetry (DSC) analyses of the films were obtained using Perkin–Elmer DSC Pyris

Scheme 2 Synthesis of carbonate modified CSBO and CPPG resins

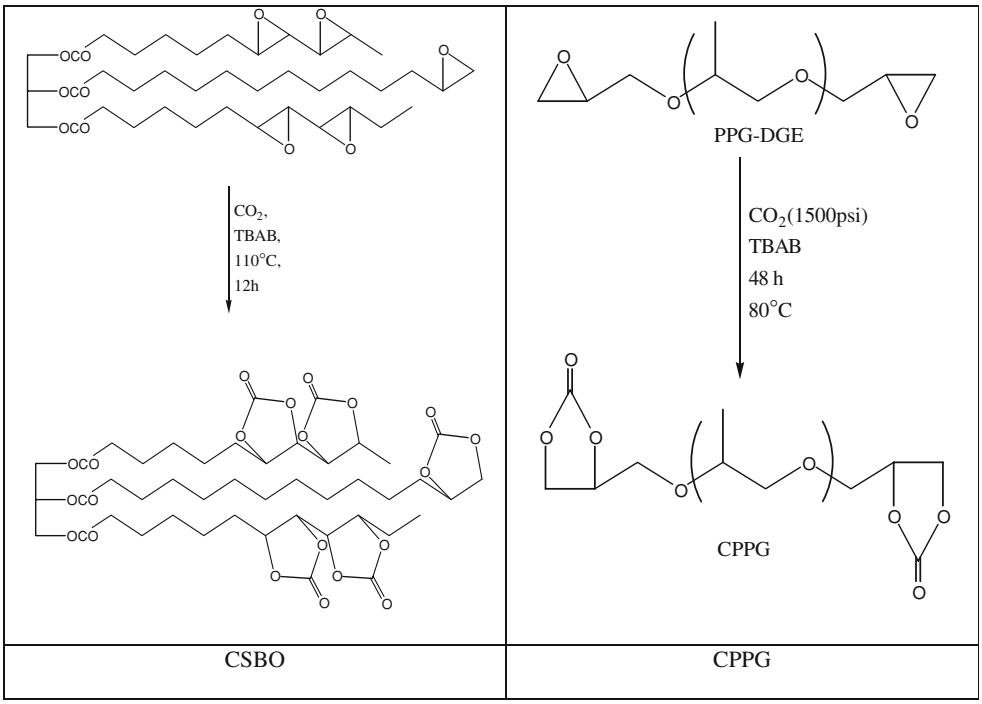

Table 2 Polyurethane–silica nanocomposite coating formulations

Sample	% Silica	M4CPS (g)	BYK[a] (mL)	CSBO (g)	CPPG (g)	BDA (g)	Pyridine[b] (mL)
CSBO-CPPG-0	0	–	2.5	15.0	15.0	5.13	5.0
CSBO-CPPG-05	0.5	0.15	2.5	15.0	15.0	5.14	5.0
CSBO-CPPG-1	1.0	0.30	5.0	15.0	15.0	5.15	5.0
CSBO-CPPG-2	2.0	0.60	10	15.0	15.0	5.16	5.0
CSBO-CPPG-4	4.0	1.20	20	15.0	15.0	5.17	5.0
CSBO-0	0	–	2.5	30.0	–	5.74	5.0
CSBO-05	0.5	0.15	2.5	30.0	–	5.75	5.0
CSBO-1	1.0	0.30	5.0	30.0	–	5.76	5.0
CSBO-2	2.0	0.60	10.0	30.0	–	5.77	5.0
CSBO-4	4.0	1.20	20.0	30.0	–	5.78	5.0

[a] BYK/Ethanol solution (2 wt%)

[b] Pyridine/Ethanol solution (4 wt%)

Diamond model device. Samples were run under a nitrogen atmosphere from −80 °C to +80 °C with a heating rate of 10 °C/min. The coating properties were measured in accordance with the corresponding standard test methods. This includes Gloss (ASTM D-523-80), Cross-cut (DIN 53151), impact (ASTM D-2794-82), MEK rub test (ASTM D-5402) and cupping test (DIN 53156).

The abrasion resistance of the coatings was determined by subjecting the coated substrate to a standardized Taber abrasion test (ASTM D4060). CS10 wheels were used with a 250 g load on each wheel, and the substrates were abraded cumulatively to 100 cycles.

Mechanical properties of the free films were determined by standard tensile stress–strain tests to measure the modulus (E), ultimate tensile strength (σ) and elongation at break (ε). Standard tensile stress–strain experiments were performed at room temperature on a Materials Testing Machine Z010/TN2S, using a cross-head speed of 10 mm/min.

3 Results and discussion

In this study polyurethane/silica nanocomposites were prepared by nonisocyanate route and their coating performance was investigated. Soybean oil and PPG based PU coatings were reinforced by cyclic-carbonate-modified silica nanoparticles. This new product combines the low cost advantages of vegetable oils and nanocomposite technology for getting higher performance and environmentally friendly nonisocyanate coating technology.

The morphology of prepared silica particles (M1–M5) were analyzed by SEM. The morphology of M4 particles

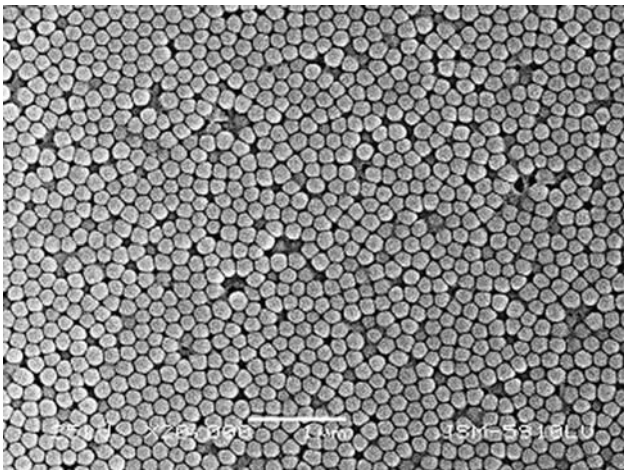

Fig. 1 SEM micrograph of M4 particles

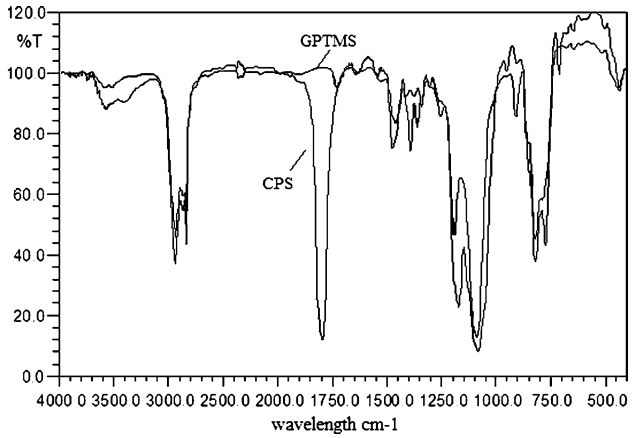

Fig. 2 FT-IR spectra of GPTMS and CPS

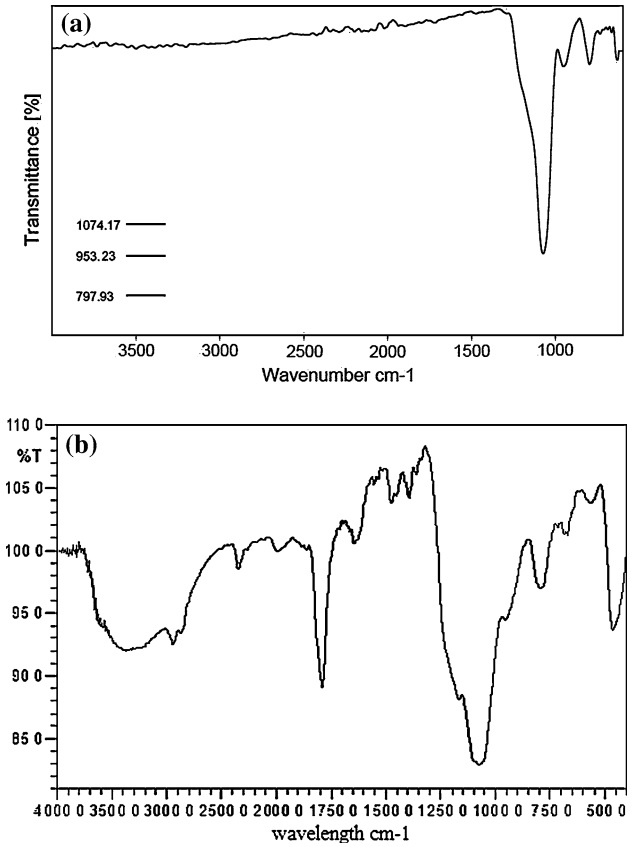

Fig. 3 FT-IR spectra of (**a**) M4; (**b**) M4CPS

was given in Fig. 1 representatively. SEM investigation demonstrated that all particles are spherical in shape as expected, the mean particle diameters were changed in the range of 165–321 nm as given in Table 1. As seen in Table 1, at constant TEOS concentration, ethanol, water and ammonia concentrations significantly affect the particle size. With increasing the concentration of ammonia the particle size increases. Matsoukas and Gulari reported that ammonia promotes hydrolysis and condensation rate, resulting in faster kinetics and larger particles [41]. On the other hand at constant ammonia concentration, a decrease in the particle size of silica particles from 321 nm to 237 nm with decreasing water concentration from 80 mM to 40 mM can be seen. It was reported previously that in the presence of high water concentration, a lots of subparticles are produced due to higher nucleation rate and the strong hydrogen bonding between them leads to agglomeration. As a result larger particles are obtained at higher water concentration [42–44]. For surface modification we chose the particles M4 due to their relatively smaller size (165 nm), perfect spherical shape and homogeneity.

The carbonate functional silane-coupling agent (CPS) synthesized from GPTMS. Synthesis process was followed by FT-IR (Fig. 2). The peak that is not present in GPTMS spectrum, but persists in CPS spectrum intensively at 1,797 cm^{-1} was attributed to the carbonyl of cyclic carbonate structure and the one which is present in GPTMS spectrum, but disappeared in CPS spectrum at 906 $cm^{-1,}$ was attributed to epoxy groups. From these results it is concluded that CPS synthesis was achieved successfully.

Figure 3a and b show the FT-IR spectra of silica particles (M4) and carbonate functional silica particles (M4CPS), respectively. In Fig. 3b, the peak at 1,792 cm^{-1} was attributed to carbonate carbonyl so that the existence of carbonate groups on the particles has been proved. Scheme 1 depicts the synthesis route of M4CPS. In surface modification CPS acts as a coupling agent bearing reactive carbonate groups. Here the coupling molecule allows the anchoring of carbonate groups to the inorganic silica surface. In this case the bonding results from the facile formation of strong Si–O–Si bonds between the inorganic phase and organosilane. The carbonate modification of the silica surface was investigated by TGA analysis. Figure 4 shows that, 21 wt% of weight loss is related with organic part and the residual part (79 wt%) is due to the silicon dioxide.

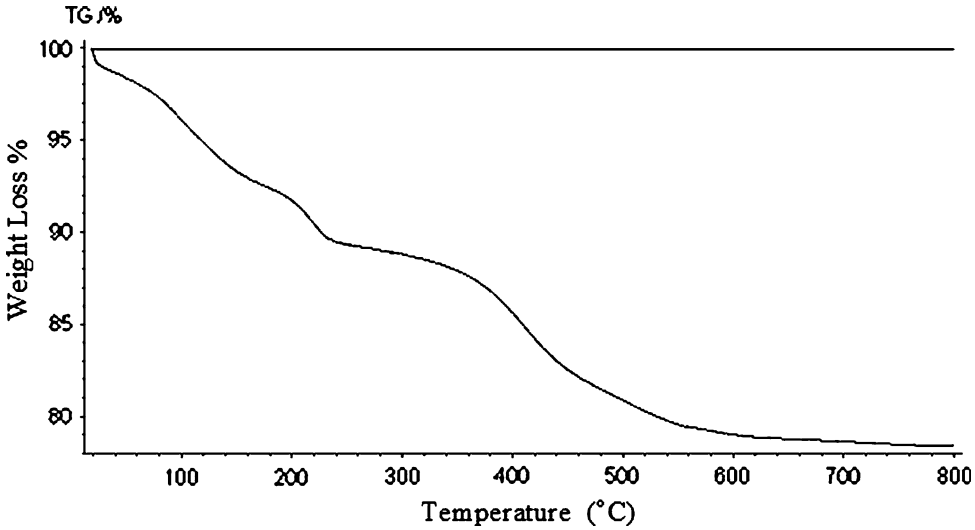

Fig. 4 TGA thermogram of M4CPS

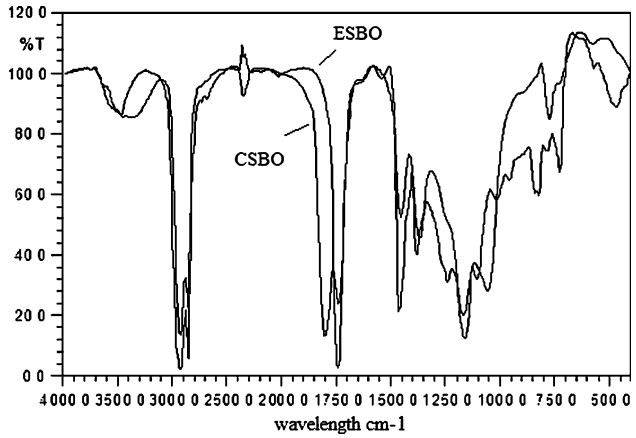

Fig. 5 FT-IR spectra of ESBO and CSBO

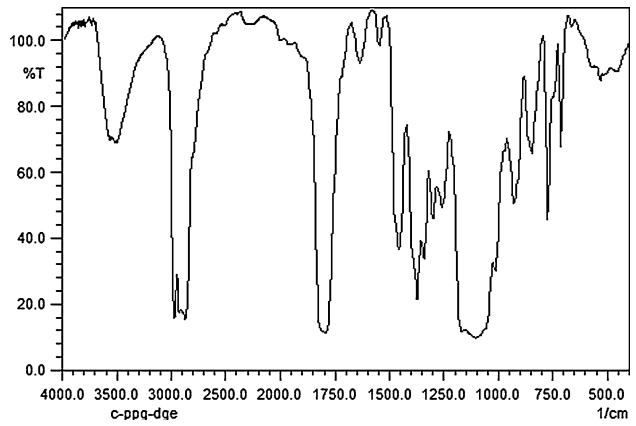

Fig. 6 FT-IR spectrum of CPPG

On the other hand, the carbon dioxide addition to ESBO and PPG-DGE oxirane groups were followed and characterized by FT-IR (Figs. 5 and 6) and ^{13}C-NMR (Fig. 7), respectively. Scheme 2 depicts the synthesis route of CSBO and CPPG resins. As can be seen from Fig. 5 the adsorption band at 1,805 cm^{-1} was attributed to cyclic carbonate group and the ones at 817 and 841 cm^{-1} were attributed to epoxy group, that means all epoxy groups were converted into cyclic carbonate structure. In addition in Fig. 6, the characteristic peak for cyclic carbonate functionality was observed at 1,800 cm^{-1}. Figure 7 shows the ^{13}C-NMR spectra of the CPPG resin. Three peaks are evident in the ^{13}C-NMR spectra, an increase in the intensity of the peak at 155 ppm from carbonyl carbon of cyclic carbonate and decrease in the intensity of the peaks at 44 and 52 ppm from carbon atoms of epoxy structure prove a successfully synthesized of cyclic carbonate resin (CPPG)[33].

A total of 10 different coating formulations were prepared by mixing appropriate amounts of carbonate resins with amine crosslinker. In the formulations CSBO resin and CSBO-CPPG resin mixture (50:50 wt%) were used to obtain organic matrix. To overcome poor dispersion of silica particles in the hydrophobic CSBO resin, mixture comprised of CSBO and CPPG with equal weight ratios were prepared. Single phase resin mixture were prepared and used in the formulations. Non-isocyanate polyurethane nanocomposite coatings on aluminum panels were prepared by thermal curing method and characterized. The feed compositions are collected in Table 2.

The thermal properties of the hybrid coatings were characterized by DSC and TGA analyses. In Fig. 8a, b the DSC thermograms can be seen and evaluated data were listed in Table 3. As it is shown in Fig. 8a, the CSBO based coating have a single T_g around −15.2 °C and a narrow endotherm at 60.7 °C. The melting peak can be attributed to the orientation of fatty acid units in the structure. The incorporation of silica does not make significant effect on T_g and T_m values. However as seen in Table 3, the T_g values of silica containing CSBO-CPPG based coatings

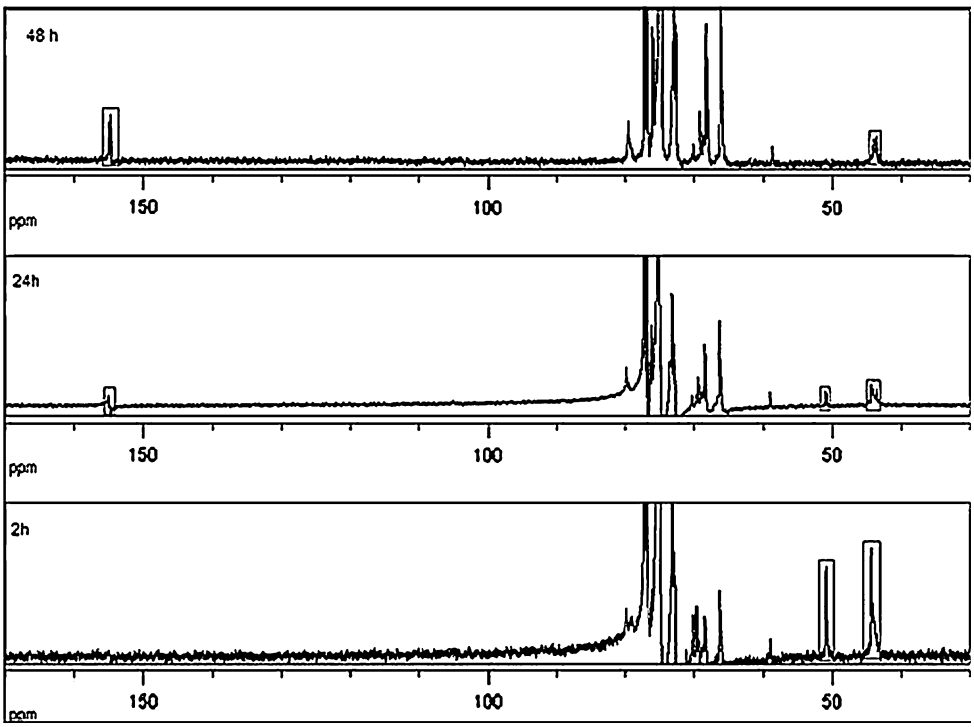

Fig. 7 ^{13}C-NMR spectra of CPPG

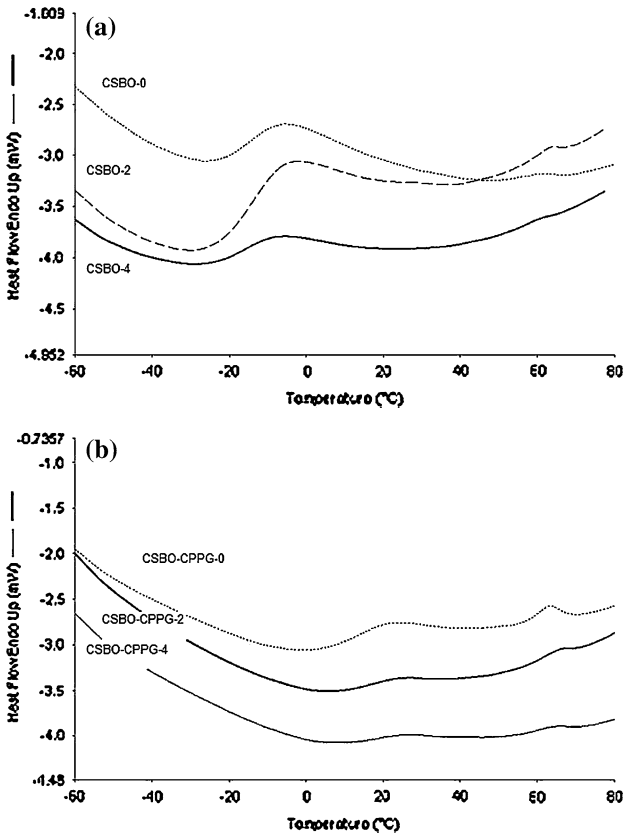

Fig. 8 DSC curves for (**a**) CSBO based nanocomposite and (**b**) CSBO-CPPG based nanocomposite coatings

Table 3 DSC analysis of CSBO and CSBO-CPPG based nanocomposite coatings

	T_g (°C)	T_m (°C)	ΔH melting (J/g)
CSBO-0	−15.2	60.7	0.079
CSBO-2	−15.4	63.3	0.196
CSBO-4	−15.7	60.0	0.041
CSBO-CPPG-0	13.3	63.1	0.649
CSBO-CPPG-2	18.6	60.1	0.155
CSBO-CPPG-4	18.9	59.5	0.119

shifts 5 °C approximately from 13 °C to 18 °C. Moreover, the CSBO and CPPG resin mixture shows only single T_g which demonstrates the compatibility of two resins. For CSBO-CPPG based coatings, the decrease in ΔH (enthalpy of melting) shows that the crystallinity may be influenced strongly by the silica amount.

TGA analyses were conducted for the formulation, which contains 0, 1, and 4% (wt) silica particles in air atmosphere. The evaluations of the thermograms are shown in Table 4. One can see that all samples exhibited 5 wt% weight loss between 125 °C and 170 °C. This could result from evaporation of alcohol or moisture adsorbed on silica particles and the excess amount of BDA and pyridine used while curing. On the other hand, the formulations, which consist of only CSBO, are degraded at single step, whereas the formulations consist of CSBO-CPPG are degraded in a

Table 4 TGA analyses of free films

	5 wt% weight loss (°C)	Max weight loss (°C)	2nd weight loss (°C)	Char yield (%)
CSBO-0	125	345	–	0.4
CSBO-1	120	345	–	1.3
CSBO-4	125	350	–	3.2
CSBO-CPPG-0	145	330	435	0
CSBO-CPPG-1	170	360	435	1.6
CSBO-CPPG-4	145	370	–	3.0

two-step manner. Neat CSBO coating is degraded at 345 °C and CSBO-CPPG coating is degraded at 330 and 435 °C. It is assumed that, the first weight loss at 330 °C belongs to CSBO units while the second weight loss at 435 °C may be due to the CPPG structure [45]. The maximum weight loss temperature for 4 wt% silica particles containing CSBO is shifted to 350 °C. Furthermore, though CSBO-CPPG-0 degrades in two steps, CSBO-CPPG-4 degrades interestingly in a single step. The positive effect of modified silica particles on single step degradation of CSBO-CPPG system could be explained in such a way that PPG chains are able to disperse particles in the medium throughout the interactions between ether linkages and silanol groups. The compatibility of the CPS, CSBO and CPPG system increases. Therefore better interaction on the molecular level was attained after crosslinking reaction. Eventually, the maximum weight loss at 330 °C was raised to 370 °C.

Figure 9a, b show the trend of tensile strength, elongation at break and Young modulus of CSBO and CSBO-CPPG based PU nanocomposite coatings. The evaluated data was listed in Table 5. Young's modulus and stress at break of CSBO formulations increased up to 2 wt% silica content, but decreased with the addition of 4 wt%. Silica content has no considerable effect on elongation at break. This material shows stronger and harder properties with increasing silica content. However with further increase in silica content, silica aggregates makes the coating brittle. In the formulations prepared by CSBO-CPPG, while silica has no effect on Young's modulus, it increased elongation. It is assumed that the compatibility between silica and polypropylene glycol structure is higher than soy bean oil based resin. Silica particles disperse better in the CSBO-CPPG resin and they behaves as a filling material by increasing the impact strength of the coating. Overall, more durable and ductile materials were achieved.

The coated aluminum panels were subjected to performance tests, which are gloss, Taber abrasion, impact, cupping, cross-cut and MEK rubbing. These results are shown in Table 6. Each result reported is an average of four separate measurements performed. After impact and

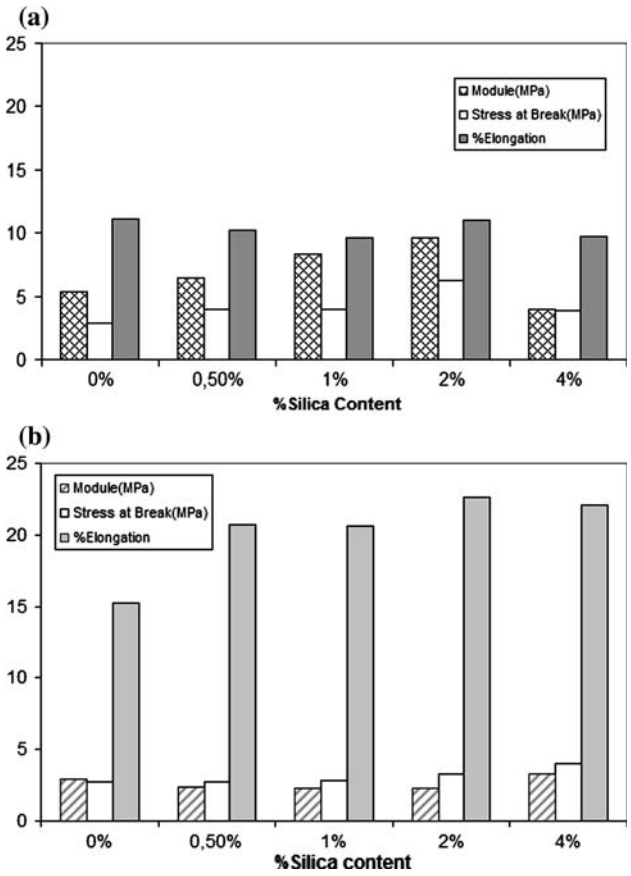

Fig. 9 Stress–Strain data for (**a**) CSBO and (**b**) CSBO-CPPG free films

Table 5 Stress–strain analysis of coatings

	Young modulus, MPa	Stress at break, MPa	% Elongation
CSBO-0	5.31	2.87	11.12
CSBO-05	6.43	3.93	10.21
CSBO-1	8.34	4.01	9.60
CSBO- 2	9.66	6.25	11.06
CSBO-4	3.97	3.87	9.75
CSBO-CPPG-0	2.90	2.77	15.26
CSBO-CPPG-05	2.39	2.77	20.73
CSBO-CPPG-1	2.25	2.79	20.61
CSBO-CPPG-2	2.29	3.27	22.61
CSBO-CPPG-4	3.29	4.03	22.08

cupping tests applied on coated panels, no damage could be seen on coatings. In cupping tests, at the moment that the Aluminum panels itself begins to break off, the polymeric coating stays still. This would indicate that films tend to be hard and strong [14]. The cross-cut adhesion experiments showed that 100% adhesion was reached for all coating compositions. As can be seen in Table 4, the gloss of

Table 6 Physical and mechanical characterizations of coatings

	Gloss (20°)	Taber abrasion[a]	Impact strength[b]	Cupping	Cross-cut	MEK rubbing
CSBO-0	82	6.5 ± 0.3	No damage	No damage	5B	200
CSBO-05	75	6.0 ± 0.3	No damage	No damage	5B	300
CSBO-1	65	6.1 ± 0.2	No damage	No damage	5B	330
CSBO-2	64	5.7 ± 0.2	No damage	No damage	5B	350
CSBO-4	48	6.0 ± 0.1	No damage	No damage	5B	400+
CSBO-CPPG-0	51	21 ± 0.2	No damage	No damage	5B	80
CSBO-CPPG-05	71	16.6 ± 0.4	No damage	No damage	5B	100
CSBO-CPPG-1	76	15.3 ± 0.3	No damage	No damage	5B	120
CSBO-CPPG-2	75	7 ± 0.4	No damage	No damage	5B	180
CSBO-CPPG-4	70	12.9 ± 0.2	No damage	No damage	5B	190

[a] mg weight loss for 100 cycle

[b] Dropping 1 kg weight over 1 m

coatings, for CSBO formulations taken at 20° decreases steadily with increasing silica content, whereas the measured values for CSBO-CPPG resin combinations increased up to 1 wt% silica content. At higher contents, gloss does not affected appreciably. For CSBO system the decrease in gloss may be attributed to phase separation between silica particles and organic coating.

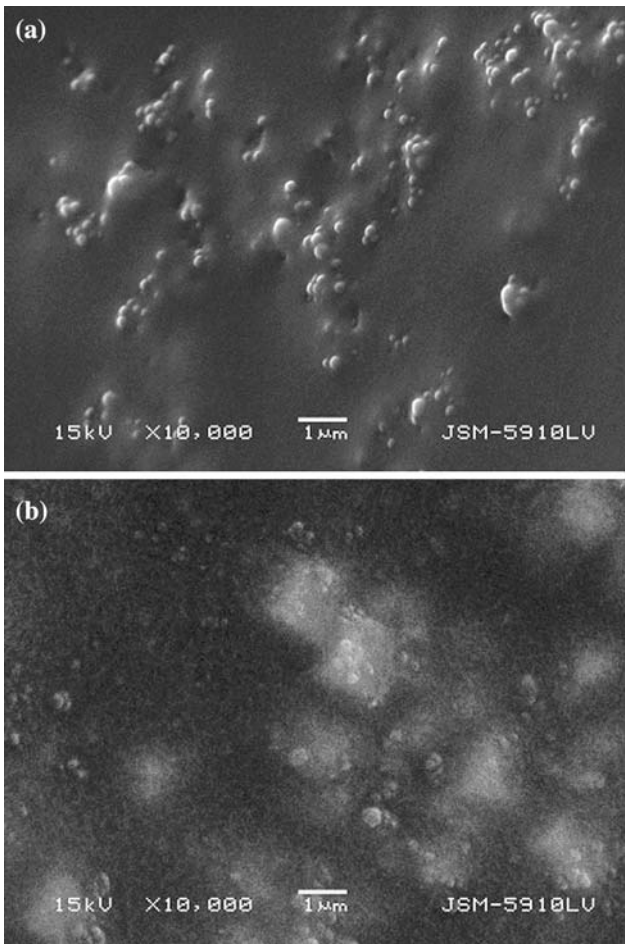

Fig. 10 SEM images of (**a**) CSBO-CPPG-1 and (**b**) CSBO-1 films

The solvent resistance of coatings was also examined by performing MEK rubbing test. CSBO coatings with 4 wt% silica content were unaffected by 400 double rubs. As can be seen in Table 6, CSBO coating resistance to MEK double rubs increase with silica contents. MEK rub resistance may also give an some indication of the degree of curing of a coating.

In Taber abrasion tests silica could not significantly affect the abrasion resistance of CSBO system. However, an increase in abrasion resistance of CSBO-CPPG system up to 2 wt% silica was observed, afterwards the resistance decreased again.

Figure 10a, b show the surface morphology of the hybrid material; CSBO-CPPG-1, and CSBO-1, respectively. SEM analyses of composite materials showed that, soybean oil based polyurethane fails to disperse the silica particles comparing to CPPG based one. The aggregation and phase separation can be seen in the case of CSBO based polyurethane–silica coating.

4 Conclusions

In this paper, environmentally friendly polyurethane–silica nanocomposite coatings were developed. The silica particles about 150–200 nm in size were prepared successfully. In addition, the synthesis of cyclic carbonate functional alkoxysilane (4-((3-(trimethoxysilyl)propoxy)methyl)-1,3-dioxolan-2-one, CPS) was reported firstly in this paper. CPS was used to modify the surface of silica particles and used as a coupling agent to improve the compatibility of the organic phase and silica particles. The nonisocyanate based polyurethane/silica nanocomposite coatings based on cyclic carbonate functional soybean oil and polypropylene glycol resins were prepared and their coating performance was investigated. No demage was observed in the impact strength of the coatings. The gloss of CSBO based coatings, decreased steadily with increasing silica content and

it was attributed to the compatibility problem between inorganic and organic phases. Moreover with the addition of CPPG into the formulation, the problem on gloss was solved. The DSC studies also demonstrated that CSBO and CPPG segments are compatible and has a single T_g around 13 °C. The morphology studies indicate cyclic-carbonate-modified silica nanoparticles could be dispersed in CPPG-containing formulations better than soybean oil based formulations and in this way the thermal, mechanical, and coating properties of CSBO-CPPG based PU/silica nanocomposite coatings are improved as well.

Acknowledgements This work was supported by TUBITAK (The Scientific&Technological Research Council of Turkey) Research Project under grant Project Number: 106T083. The authors are pleased to acknowledge Mustafa Ilhan for SEM and BurcinYıldız for NMR analyses.

References

1. Kickelbick G (2003) Prog Polym Sci 28:83
2. Bauer F, Flyunt R, Czihal K, Ernst H, Naumov S, Buchmeiser MR (2007) Nucl Instrum Methods Phys Res B 265(1):87
3. Chen Y, Kim H (2007) Mater Lett 61:5040
4. Gun'ko VM, Borysenko MV, Pissis P, Spanoudaki A, Shinyashiki N, Sulim IY, Kulik TV, Palyanytsya BB (2007) Appl Surf Sci 253:7143
5. Lai YH, Kuo MC, Huang JC, Chen M (2007) Mater Sci Eng A 458:158
6. Bongiovanni R, Sangermano M, Ronchetti S, Priola A, Malucelli G (2007) Polymer 48:7000
7. Kojima Y, Usuki A, Kawasumi M, Okada A, Fukushima Y, Kurauchi T, Kamigaito O (1993) J Mater Res 8:1174
8. Yuan J, Zhou S, Gu G, Wu L (2005) J Mater Sci 40:3927
9. Rong MZ, Zhang MQ, Zheng YX, Zeng HM, Walter R, Friedrich K (2001) Polymer 42:167
10. Yano K, Usuki A, Okada A (1997) J Polym Sci Part A: Polym Chem 35:2289
11. Wang S, Hu Y, Lin Z, Zhou G, Wang Z, Chen Z, Fan W (2003) Polym Int 52:1045
12. Liu Y-L, Hsu C-Y, Hsu K-Y (2005) Polymer 46:1851
13. Sun Y, Zhang Z, Wong CP (2005) J Colloid Interf Sci 292:436
14. Kahraman MV, Kuğu M, Menceloğlu Y, Kayaman-Apohan N, Güngör A (2006) J Non-Cryst Solids 352:2143
15. Bayramoğlu G, Kahraman MV, Kayaman-Apohan N, Güngör A (2007) Prog Org Coat 57:50
16. Karatas S, Kayaman-Apohan N, Demirer H, Gungor A (2007) Polym Advan Technol 18:490
17. Karatas S, Hosgor Z, Menceloglu Y, Kayaman-Apohan N, Gungor A (2006) J Appl Polym Sci 102:1906
18. Figovsky OL, Shapovalov LD (2002) Macromol Symp 187:325
19. Ochiai B, Endo T (2005) Prog Polym Sci 30:183
20. Baba A, Nozaki T, Matsuda H (1987) Bull Chem Soc Jpn 60:1552
21. Srivastava R, Srinivas D, Ratnasamy P (2005) J Catal 233:1
22. Kiharat N, Endo T (1994) Macromolecules 27:6239
23. Webster DC, Crain AL (2000) Prog Org Coat 40:275
24. Park D-W, Mun N-Y, Kim K-H, Kim I, Park S-W (2006) Catal Today 115:130
25. Omae I (2006) Catal Today 115:33
26. Park D-W, Moon JY, Yang JG, Lee JK (1997) Energy Convers Manage 38:449
27. Zhang X, Wei N, Sun Y (2006) Catal Today 115:102
28. Ono F, Qiao K, Tomida D, Yokoyama C (2006) J Mol Cata A: Chem 263:223
29. Sun J, Fujita S-I, Arai M (2005) J Organomet Chem 690:3490
30. Sakai T, Kihara N, Endo T (1995) Macromolecules 28:4701
31. Wang J-Q, Kong D-L, Chen J-Y, Cai F, He L-N (2006) J Mol Catal A: Chem 249:143
32. Parzuchowski PG, Jurczyk-Kowalska M, Ryszkowska J, Rokicki G (2006) J Appl Polym Sci 102:2904
33. Tamami B, Sohn S, Wilkes GL (2004) J Appl Polym Sci 92:883
34. Webster DC (2003) Prog Org Coat 47:77
35. Rokicki G, Wojciechowski C (1990) J Appl Polym Sci 41:647
36. Bürgel T, Fedtke M (1993) Polym Bull 30:61
37. Ochıaı B, Inoue S, Endo T (2005) J Polym Sci Part A: Polym Chem 43:6613
38. Van Holen J (2004) US Patent 2004/0236119
39. Figovsky O, Shapovalov L, Buslov F (2005) Surf Coat Int B: Coat Trans 88:67
40. Stöber W, Fınk A, Bohn E (1968) J Colloid Interf Sci 26:62
41. Matsoukas T, Gulari E (1988) J Colloid Interf Sci 124:252
42. Rao KS, El-Hami K, Kodaki T, Matsushige K, Makino K (2005) J Colloid Interf Sci 289:125
43. Park SK, Kim KD, Kim HT (2002) Colloids Surf A 197:7
44. Costa CAR, Leite CAP, Galembeck F (2003) J Phys Chem B 107:4747
45. Chang K-C, Chen Y-K, Chen H (2007) Surface Coat Technol 201:957